第 34 卷第 5 期
2018 年 5 月

无 机 化 学 学 报
CHINESE JOURNAL OF INORGANIC CHEMISTRY

Vol.34 No.5
997-1006

杂双金属 Cu(Ⅱ)-Nd(Ⅲ)和 Zn(Ⅱ)-Ce(Ⅲ)的 Salamo 型配合物：合成、晶体结构和荧光性质

杨玉华 张 雨 于 盟 郑姗姗 董文魁*
(兰州交通大学化学与生物工程学院，兰州 730070)

摘要：合成了 2 个异双核金属 Salamo 型配合物 [Cu(L)Nd(NO$_3$)$_3$(C$_2$H$_5$OH)] (**1**)和[Zn(L)(OAc)Ce(NO$_3$)$_2$(CH$_3$OH)] (**2**)(H$_2$L=*O*,*O*′-(ethane-1,2-diyl)bis(1-(3-ethoxy-2-hydroxyphenyl)-3-ethoxy-2-hydroxybenzaldehyde oxime))，并通过元素分析、红外、紫外、荧光光谱和 X 射线晶体学对其进行了表征。配合物 **1** 是不对称的双核结构，其中 Cu(Ⅱ)原子为五配位具有稍微扭曲的四方锥几何构型，而钕(Ⅲ)原子是十配位具有一种扭曲的双帽十二面几何构型。配合物 **2** 也是不对称的双核结构，其 Zn(Ⅱ)原子为五配位具有一种介于四方锥和三角双锥体之间的几何构型，Ce(Ⅲ)原子为十配位采用了一种扭曲的双面十二面几何构型。与配体相比，在激发波长为 318 nm 时配合物 **1** 发生了荧光淬灭，而配合物 **2** 表现出荧光增强。

关键词：Salamo 型配体；3*d*-4*f* 配合物；合成；晶体结构；荧光性质
中图分类号：O614.121；O614.33$^+$5；O614.24$^+$1；O614.33$^+$2　　**文献标识码**：A　　**文章编号**：1001-4861(2018)05-0997-10
DOI：10.11862/CJIC.2018.125

Heterobimetallic Cu(Ⅱ)-Nd(Ⅲ) and Zn(Ⅱ)-Ce(Ⅲ) Salamo-Type Complexes: Syntheses, Crystal Structures and Fluorescence Properties

YANG Yu-Hua　ZHANG Yu　YU Meng　ZHENG Shan-Shan　DONG Wen-Kui*
(*School of Chemical and Biological Engineering, Lanzhou Jiaotong University, Lanzhou* 730070, *China*)

Abstract: Heterobinuclear 3*d*-4*f* complexes having chemical formulae [Cu(L)Nd(NO$_3$)$_3$(C$_2$H$_5$OH)] (**1**) and [Zn(L)(OAc)Ce(NO$_3$)$_2$(CH$_3$OH)] (**2**) with a Salamo-type ligand *O*,*O*′-(ethane-1,2-diyl)bis(1-(3-ethoxy-2-hydroxyphenyl)-3-ethoxy-2-hydroxybenzaldehyde oxime) (H$_2$L)were synthesized, and characterized by elemental analyses, IR, UV-Vis, fluorescence spectra and X-ray crystallography. Complex **1** is an asymmetrical dinuclear complex, the pentacoordinate Cu(Ⅱ) ion has a slightly distorted square pyramidal geometry, and deca-coordinated Nd(Ⅲ) ion possesses a distorted bicapped twelve surface geometry. Complex **2** is also an asymmetrical dinuclear complex, the penta-coordinate Zn(Ⅱ) ion bears a distorted square pyramidal geometry too, and deca-coordinated Ce(Ⅲ) ion adopts a distorted bicapped twelve surface geometry. Compared with the ligand H$_2$L, complex **1** showed fluorescence quenching, while complex **2** exhibited the fluorescence enhancement when the excitation wavelength is 318 nm. CCDC: 1815944, **1**; 1815943, **2**.

Keywords: Salamo-type ligand; 3*d*-4*f* complex; synthesis; crystal structure; fluorescence property

收稿日期：2018-01-10。收修改稿日期：2018-03-16。
国家自然科学基金(No.21361015，21761018)资助项目。
*通信联系人。E-mail：dongwk@126.com；会员登记号：02M87091161。

0 Introduction

Much recent interests have been focused on 3d transition metal complexes with Salen-[1-7] or Salamo-type[8-12] ligands, which have potential applications, such as luminescent[13-19] and magnetic[20-25] materials, supramolecular architectures[26-31], biological fields[32-39], molecular recognitions[40-43] and electrochemistries[44-45]. Because of the high coordination ability of phenoxy groups, many central metals can be coordinated to form heteronuclear metal complexes[46-50].

Because the *f-f* transitions of lanthanide ions are parity forbidden, the absorption coefficients are very low and the emissive rates are slow[51], suitable organic ligands must be well-designed to strengthen luminescent intensity, which act as sensitizers to excite lanthanide ions (antenna effect)[52].

Herein, two kinds of hetero-bimetallic 3*d*-4*f* complexes containing a Salamo-type ligand *O*,*O*′-(ethane-1, 2-diyl)bis(1-(3-ethoxy-2-hydroxyphenyl)-3-ethoxy-2-hydroxybenzaldehyde oxime) (H_2L) were synthesized and structurally characterized. Furthermore, their fluorescence properties were investigated.

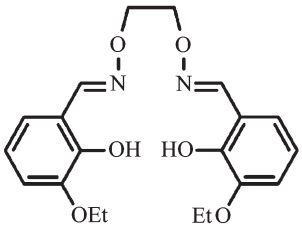

Scheme 1 Structure of the ligand H_2L

1 Experimental

1.1 Materials and physical measurements

3-Ethoxybenzaldehyde (99%) was purchased from Alfa Aesar and used without further purification. Ethanol and methanol and other reagents and solvents were analytical grade reagents from Tianjin Chemical Reagent Factory. C, H and N analyses were obtained using a GmbH VarioEL V3.00 automatic elemental analysis instrument. Elemental analyses for metals were monitored with an IRIS ER/S-WP-1 ICP atomic emission spectrometer. Melting points were acquired by the use of a microscopic melting point apparatus made in Beijing Taike Instrument Limited Company and were uncorrected. IR spectra were recorded on a Vertex70 FT-IR spectrophotometer, with samples prepared as KBr (500~4 000 cm^{-1}). UV-Vis absorption spectra were recorded on a Shimadzu UV-3900 spectrometer. Fluorescence spectra in solution were recorded on a Hitachi F-7000 spectrometer. ^1H NMR spectra were determined by a German Bruker AVANCE DRX-400 spectrometer.

1.2 Synthesis and characterization of H_2L

The Salamo-type ligand H_2L was synthesized according to an analogous method reported earlier[53]. A solution of 1,2-bis(aminooxy)ethane (276.0 mg, 3.0 mmol) in ethanol (10 mL) was added to a solution of 3-ethoxybenzaldehyde (996.0 mg, 6.0 mmol) in ethanol (20 mL), and the mixture was heated at 55~60 ℃ for 5h. After cooling to room temperature, the precipitate was filtered off, and white crystalline H_2L was obtained. Yield: 784.0 mg, 67.3%. m.p. 462~463 K. Anal. Calcd. for $C_{20}H_{24}N_2O_6$(%): C, 61.84; H, 6.23; N, 7.21. Found (%): C, 61.80; H, 6.30; N, 7.19. ^1H NMR (400 MHz, $CDCl_3$): δ 1.47 (t, J=4 Hz, 6H, CH_3), 4.11 (dd, J=4, 8 Hz, 4H, CH_2), 4.46 (s, 4H, CH_2), 6.82 (m, 3H, ArH), 6.88 (m, 3H, ArH), 8.26 (s, 2H, CH=N), 9.68 (s, 2H, OH). IR (KBr, cm^{-1}): 1 611 ($\nu_{C=N}$), 1 248 (ν_{Ar-O}). UV-Vis (MeCN, 10 μmol·L^{-1}), λ_{max}/nm: 270, 319.

1.3 Synthesis of complex 1

The ligand H_2L (19.4 mg, 0.05 mmol) was dissolved in 5 mL of ethanol and stirred with ethanol solution (5 mL) of $Cu(OAc)_2·2H_2O$ (10.3 mg, 0.05 mmol) and $Nd(NO_3)_3·6H_2O$ (22.6 mg, 0.05 mmol), filtered to get a dark green solution. Through partial solvent evaporation, single crystals suitable for X-ray diffraction analysis were obtained after several days. Yield: 60.3%. Anal. Calcd. for $C_{22}H_{28}NdCuN_5O_{16}$(%): C, 31.98; H, 3.42; N, 8.48. Found(%): C, 32.24; H, 3.29; N, 8.43.

1.4 Synthesis of complex 2

The synthesis of complex **2** is similar to that of complex **1**, except that the solvent is replaced. The ligand was dissolved in acetone, while the metal salts $Zn(OAc)_2$ and $Ce(NO_3)_3$ were dissolved in methanol. White crystals of complex **2** were collected. Yield: 58.6%. Anal. Calcd. for $C_{23}H_{29}CeZnN_4O_{15}$(%): C, 34.23;

H, 3.62; N, 6,94. Found(%): C, 34.39; H, 3.47; N, 6.82.

1.5 X-ray crystallography

The single crystals of complexes **1** and **2** were placed on a Super Nova Dual Eos four-circle diffractometer. The diffraction data were collected using a graphite monochromated Mo $K\alpha$ radiation (λ=0.710 73 nm). Data collection and reduction were performed using CrysAlisPro and then processed with Olex2. The structures were solved with SHELXS-2008 and refined with SHELXL-2014[54]. All non-hydrogen atoms were refined anistropically and hydrogen atoms were added in calculated positions and refined using a riding model. The crystallographic data and structural refinements for complexes **1** and **2** are listed in Table 1.

CCDC: 1815944, **1**; 1815943, **2**.

Table 1 Crystallographic data and refinement parameters for complexes 1 and 2

Complex	1	2
Empirical formula	$C_{22}H_{28}NdCuN_5O_{16}$	$C_{23}H_{29}CeZnN_4O_{15}$
Formula weight	826.27	806.99
Crystal system	Monoclinic	Triclinic
Space group	$P2_1/n$	$P\bar{1}$
a / nm	0.942 91(3)	0.905 77(8)
b / nm	1.528 96(4)	1.203 32(13)
c / nm	2.135 12(4)	1.547 57(13)
α / (°)		99.496(8)
β / (°)	92.353(2)	102.562(7)
γ / (°)		111.854(9)
V / nm^3	3.075 55(14)	1.470 7(3)
Z	4	2
D_c / (g·cm^{-3})	1.784	1.822
μ / mm^{-1}	2.441	2.422
F(000)	1 648	806
Crystal size / mm	0.24×0.22×0.15	0.21×0.14×0.12
θ range / (°)	3.43~26.02	3.52~26.02
Limiting indices	$-11 \leqslant h \leqslant 9, -13 \leqslant k \leqslant 18, -16 \leqslant l \leqslant 26$	$-11 \leqslant h \leqslant 11, -14 \leqslant k \leqslant 11, -19 \leqslant l \leqslant 18$
Independent reflection	6 053	5 765
Completeness to θ / %	99.68	99.75
Data, restraint, parameter	6 053, 30, 434	5 765, 3, 404
GOF on F^2	1.035	1.026
Final R indices [$I>2\sigma(I)$]	R=0.035 2, wR=0.058 7	R=0.034 5, wR=0.064 9
Largest diff. peak and hole / (e·nm^{-3})	650 and −510	470 and −840

2 Results and discussion

2.1 IR spectra

IR spectra of H_2L and its corresponding complexes **1** and **2** exhibited various bands in the region of 4 000~400 cm^{-1} (Fig.1). The O-H stretching band of the free ligand H_2L was observed at 2 981 cm^{-1} that belongs to the phenolic hydroxyl group, whereas complexes **1** and **2** showed a vibration band at 3 413 and 3 402 cm^{-1} that belong to coordinated ethanol or methanol molecules.

The free ligand H_2L exhibited characteristic C=N stretching band at 1 611 cm^{-1}, which is shied by 5~7 cm^{-1} in complexes **1** and **2**, respectively, indicating that the nitrogen atoms of C=N group are coordinated to the Cu (Ⅱ) or Zn (Ⅱ) ions, which is similar to previously reported metal(Ⅱ) complexes[55].

The Ar-O stretching frequency appeared at 1 248 cm^{-1} for the ligand H_2L, while the Ar-O stretching frequencies in complexes **1**, and **2** are observed at

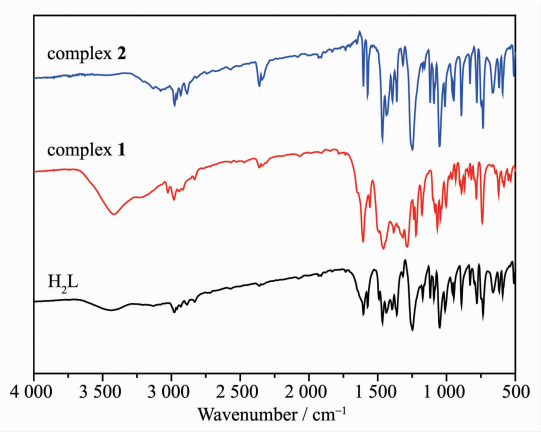

Fig.1 IR spaectra of H_2L and its complexes **1** and **2**

1 233 and 1 242 cm^{-1}, respectively. The Ar-O stretching frequencies are shifted to lower frequencies, indicating that the Cu-O or Zn-O bonds are formed between the metal (Ⅱ) ions and oxygen atoms of phenolic groups.

2.2 UV-Vis absorption spectra

The absorption spectra of H_2L and its complexes **1** and **2** in diluted acetonitrile solution are shown in Fig.2. The free ligand H_2L showed three absorption bands at 222, 270 and 319 nm. The peaks at 222 and 270 nm can be assigned to the π-π* transitions of the benzene rings and the latter peak at 319 nm can be assigned to intra-ligand π-π* transition of the oxime groups[56]. Compared with the absorption peaks of H_2L, with the emergence of the first absorption peaks at ca. 276 and 277 nm were observed in complexes **1** and **2**, respectively. These peaks are bathochromically shifted, indicating coordination of the ligand moieties with metal (Ⅱ) ions. The absorption peaks at *ca.* 270 and 319 nm were absent in complexes **1** and **2**. Meanwhile, new absorption peaks were observed at *ca.* 344 and 350 nm in complexes **1** and **2**, may be due to L→M charge-transfer transitions, which are characteristic of the transition metal complexes with Salen-type N_2O_2 coordination spheres.

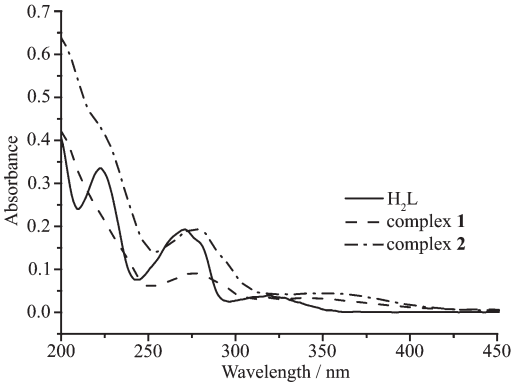

Fig.2 UV-Vis absorption spectra of H_2L and its complexes **1** and **2** in acetonitrile (10 mol·L^{-1})

2.3 Description of the crystal structures

2.3.1 Crystal structure of complex **1**

Selected bond lengths and angles for complex **1** are presented in Table 2. Complex **1** crystallizes in the monoclinic system, space group $P2_1/n$, An asymmetric unit of complex **1** includes one completely deprotonated L^{2-} unit, one Cu(Ⅲ) atom (Cu1), one Nd(Ⅲ) ion (Nd1), three NO_3^- ions and one coordinated ethanol molecule. The crystal structure of complex **1** and geometries of metal atoms are shown in Fig.3.

Cu1 atom was penta-coordinated by inner N_2O_2 (N1, N2, O1 and O5) cavity from the deprotonated L^{2-} unit and one oxygen atom (O16) of the coordinated ethanol molecule. According to the calculation of structural index parameter τ_1=0.196, Cu1 atom adopts

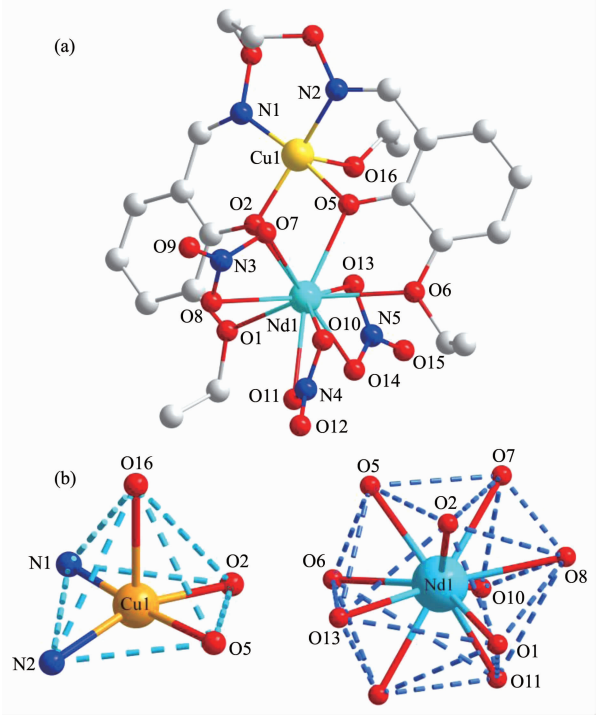

Hydrogen atoms and solvent molecules are omitted for clarity

Fig.3 (a) Molecule structure and atom numberings of complex **1** with 30% probability displacement ellipsoids; (b) Coordination polyhedron for Cu(Ⅱ) and Nd(Ⅲ) ions of complex **1**

Table 2 Selected bond lengths (nm) and angles (°) for complexes 1 and 2

1					
Nd1-O1	0.255 2(3)	Nd1-O8	0.256 8(3)	Cu1-O2	0.194 7(2)
Nd1-O2	0.240 1(2)	Nd1-O10	0.254 0(3)	Cu1-O5	0.194 1(2)
Nd1-O5	0.241 0(2)	Nd1-O11	0.255 0(3)	Cu1-O16	0.227 8(3)
Nd1-O6	0.259 7(3)	Nd1-O13	0.256 6(3)	Cu1-N1	0.194 3(3)
Nd1-O7	0.256 5(3)	Nd1-O14	0.253 8(3)	Cu1-N2	0.199 2(3)
O1-Nd1-O6	144.77(8)	O5-Nd1-O13	73.89(9)	O13-Nd1-O8	146.81(9)
O1-Nd1-O7	111.40(9)	O5-Nd1-O14	115.12(9)	O14-Nd1-O1	76.08(9)
O1-Nd1-O8	71.29(9)	O7-Nd1-O6	103.25(9)	O14-Nd1-O6	70.49(8)
O1-Nd1-O13	78.68(9)	O7-Nd1-O8	49.26(9)	O14-Nd1-O7	169.61(9)
O2-Nd1-O1	63.53(8)	O7-Nd1-O13	137.16(9)	O14-Nd1-O8	131.22(9)
O2-Nd1-O5	64.74(8)	O8-Nd1-O6	141.38(8)	O14-Nd1-O10	100.70(9)
O2-Nd1-O6	121.84(8)	O10-Nd1-O1	123.68(9)	O14-Nd1-O11	66.50(10)
O2-Nd1-O7	75.64(9)	O10-Nd1-O6	74.32(9)	O14-Nd1-O13	49.88(8)
O2-Nd1-O8	81.52(9)	O10-Nd1-O7	69.26(9)	O2-Cu1-O16	95.55(12)
O2-Nd1-O10	144.19(9)	O10-Nd1-O8	70.48(9)	O2-Cu1-N2	161.42(12)
O2-Nd1-O11	141.02(11)	O10-Nd1-O11	49.73(10)	O5-Cu1-O2	83.01(10)
O2-Nd1-O13	72.52(9)	O10-Nd1-O13	140.90(9)	O5-Cu1-O16	88.39(11)
O2-Nd1-O14	114.64(9)	O11-Nd1-O1	80.36(10)	O5-Cu1-N1	173.19(12)
O5-Nd1-O1	126.50(8)	O11-Nd1-O6	95.95(10)	O5-Cu1-N2	87.78(11)
O5-Nd1-O6	62.24(7)	O11-Nd1-O7	106.83(10)	N1-Cu1-O2	90.18(12)
O5-Nd1-O7	66.90(9)	O11-Nd1-O8	73.00(10)	N1-Cu1-O16	92.04(13)
O5-Nd1-O8	113.36(8)	O11-Nd1-O13	115.97(9)	N1-Cu1-N2	98.83(13)
O5-Nd1-O10	106.10(9)	O13-Nd1-O6	71.53(9)	N2-Cu1-O16	100.29(14)
O5-Nd1-O11	153.13(10)				
2					
Ce1-O1	0.266 4(2)	Ce1-O9	0.262 0(3)	Zn1-O2	0.199 7(3)
Ce1-O2	0.244 1(2)	Ce1-O10	0.262 4(3)	Zn1-O5	0.205 0(2)
Ce1-O5	0.243 0(3)	Ce1-O12	0.272 7(3)	Zn1-O8	0.197 4(3)
Ce1-O6	0.274 4(3)	Ce1-O13	0.256 4(3)	Zn1-N1	0.210 5(3)
Ce1-O7	0.244 4(2)	Ce1-O32	0.260 6(3)	Zn1-N2	0.206 1(3)
O1-Ce1-O6	146.10(8)	O7-Ce1-O1	127.32(8)	O13-Ce1-O10	74.20(10)
O1-Ce1-O12	69.61(9)	O7-Ce1-O6	85.03(8)	O13-Ce1-O12	48.02(10)
O2-Ce1-O1	60.92(8)	O7-Ce1-O9	141.59(10)	O13-Ce1-O32	80.10(10)
O2-Ce1-O6	124.37(8)	O7-Ce1-O10	149.63(9)	O32-Ce1-O1	71.47(8)
O2-Ce1-O7	81.56(8)	O7-Ce1-O12	112.84(9)	O32-Ce1-O6	141.20(8)
O2-Ce1-O9	84.83(9)	O7-Ce1-O13	81.42(9)	O32-Ce1-O9	145.19(9)
O2-Ce1-O10	127.05(9)	O7-Ce1-O32	63.90(9)	O32-Ce1-O10	127.23(10)
O2-Ce1-O12	124.67(9)	O9-Ce1-O1	73.88(9)	O32-Ce1-O12	66.18(9)
O2-Ce1-O13	154.73(10)	O9-Ce1-O6	73.50(9)	O2-Zn1-O5	79.75(10)
O2-Ce1-O32	75.68(9)	O9-Ce1-O10	48.14(10)	O2-Zn1-N1	87.49(12)
O5-Ce1-O1	115.68(8)	O9-Ce1-O12	104.46(10)	O2-Zn1-N2	136.25(12)
O5-Ce1-O2	64.38(8)	O10-Ce1-O1	80.85(9)	O5-Zn1-N1	160.94(12)
O5-Ce1-O6	60.13(8)	O10-Ce1-O6	70.63(9)	O5-Zn1-N2	85.54(12)

Continued Table 2

O5-Ce1-O7	71.67(9)	O10-Ce1-O12	62.27(9)	O8-Zn1-O2	110.44(11)
O5-Ce1-O9	70.04(10)	O12-Ce1-O6	110.32(8)	O8-Zn1-O5	95.00(11)
O5-Ce1-O10	108.94(9)	O13-Ce1-O1	117.54(9)	O8-Zn1-N1	102.75(12)
O5-Ce1-O12	169.71(8)	O13-Ce1-O6	72.37(9)	O8-Zn1-N2	111.73(13)
O5-Ce1-O13	126.41(10)	O13-Ce1-O9	119.81(10)	N2-Zn1-N1	94.17(13)
O5-Ce1-O32	123.37(9)				

a slightly distorted square pyramidal configuration, which N_2O_2 site occupies the basal plane and O16 is in the axial position. The bond lengths of Cu-N bonds are in the range of 0.194 3(3)~0.199 2(3) nm, and those of Cu-O bonds are in 0.194 1(2)~0.227 8(3) nm with longer bond exists in the axial position. In addition, the angles of N1-Cu1-O16 and O5-Cu1-O16 are 92.04(13)° and 88.39(11)°, respectively, nearly equal to the upright angle. Compared with crystal structures of other analogous, acetate ions no longer bridge two metal ions in a common μ_2-fashion[57] or as a terminal monodentate ligand, which does not participate in the coordination of complex **1**. Nd1 atom is deca-coordinated with outer O_4 site (O1, O2, O5 and O6) and six oxygen atoms provided by three bidentate NO_3^- ions (O7, O8, O10, O11, O13 and O14), showing a distorted bicapped twelve surface geometry. The Nd-O bond lengths are in the range of 0.240 1(2)~0.259 7(3) nm, as can be seen from Fig.3b the distances are close to each other.

2.3.2 Crystal structure of complex **2**

Selected bond lengths and angles for complex **2** are presented in Table 2. Complex **2** crystallizes in the triclinic system, space group $P\bar{1}$. The crystal structure of complex **2** and geometries of metal atoms are shown in Fig.4.

For complex **2**, an asymmetric unit includes a fully deprotonated L^{2-} unit, one Zn(Ⅱ) ion (Zn1), Ce(Ⅲ) ion (Ce1), one μ_2-acetate ion, two NO_3^- ions and one coordinated methanol molecule. Five donor atoms (N1, N2, O2, O5 and O8) of Zn1 atom come from N_2O_2 cavity and the μ_2-acetate ion, respectively. The structural index parameter τ_1 is equal to 0.412 by calculated. It is well known that the geometry of pentacoor-dinated complex is decided by geometric parameter τ, when τ=0, metal ions adopt square pyramidal configuration, when τ=1, will adopt the trigonal bipyramidal geometry. Herein, the τ value is closed to 0.5, indicating that the geometry of Zn1 atom is distorted square pyramidal configuration, where N_2O_2 are basal plane and O8 occupies the axial position. The bond lengths of Zn-N bonds are 0.206 1(3) and 0.210 5(3) nm, and those of Zn-O bonds is in the range of 0.197 4(3)~0.205 0(2) nm, which are obvious shorter than Zn-N. It is worth noting that the angle of O5-Zn1-N1 is 160.94(12)°, which is relatively close to 180°, also implying that the geometry of Zn1 atom possesses square pyramidal.

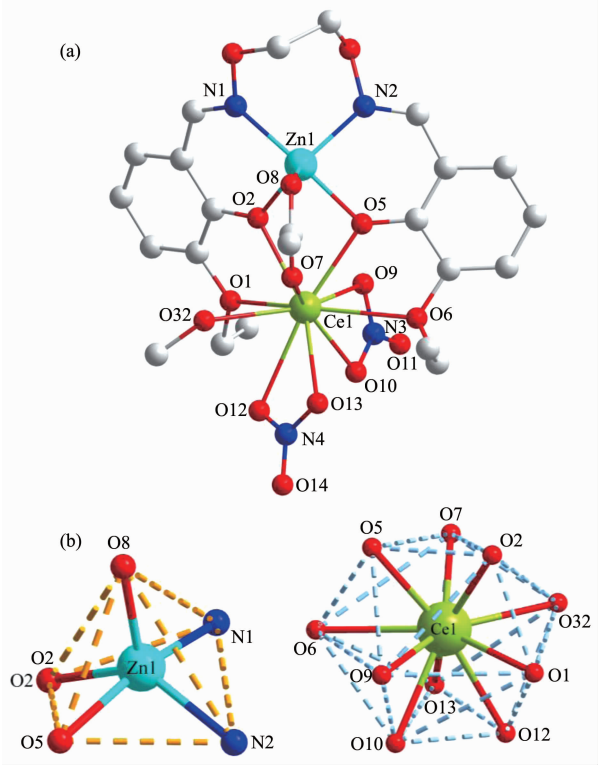

Hydrogen atoms and solvent molecules are omitted for clarity

Fig.4 (a) Molecule structure and atom numberings of complex **2** with 30% probability displacement ellipsoids; (b) Coordination polyhedron for Zn(Ⅱ) and Ce(Ⅲ) ions of complex **2**

The coordination number and geometry of Ce1 atom are same with Nd1 of complex **1**, and both of them adopt a deca-coordinated bicapped twelve surface geometry. The differences are one methanol molecule and one μ_2-acetate ion coordinated with Ce1. The bond lengths of Ce-O bonds are in the range of 0.243 0(3)~0.274 4(3) nm, while Ce1-O2 and Ce1-O5 have a shortest bond lengths and Ce1-O6 are the longest.

2.4 Supramolecular interactions

2.4.1 Supramolecular interaction of complex **1**

As shown in Fig.5 and 6, the self-assembling array of complex **1** is linked by intramolecular hydrogen bonds and intermolecular interactions. The hydrogen bond data and intermolecular interaction data are given in Table 3. In the crystal structure, there are eight intramolecular hydrogen bond

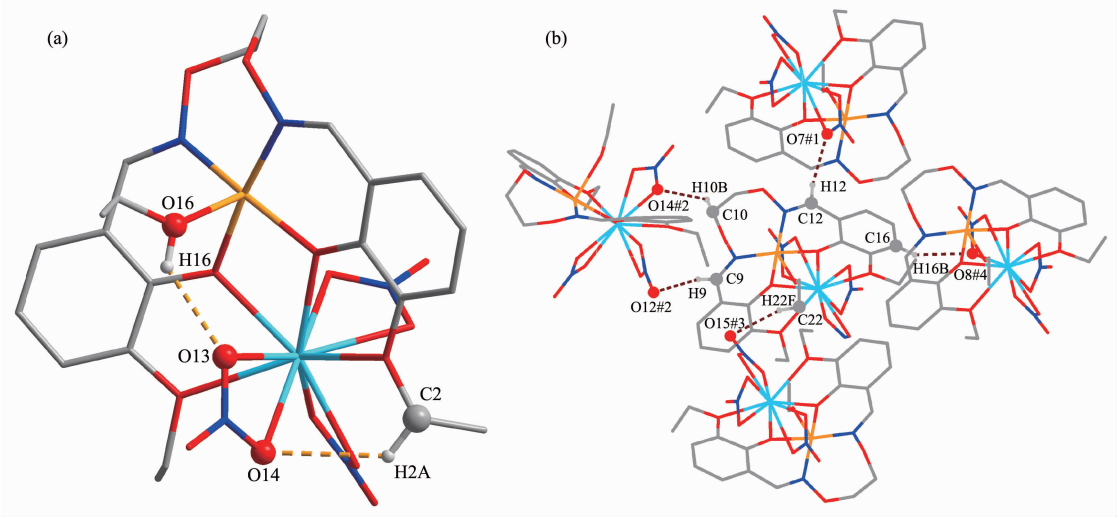

Symmetry codes: #1: 2−*x*, 2−*y*, −*z*; #2: −1/2+*x*, 3/2−*y*, −1/2+*z*; #3: 2−*x*, 1−*y*, −*z*; #4: 1+*x*, *y*, *z*

Fig.5　(a) View of the intramolecular hydrogen-bonding interactions of complex **1**; (b) View of intermolecular interactions of complex **1**

Table 3　Intra- and inter-molecular hydrogen geometries for complexes 1 and 2

Complex	D−H···A	*d*(D-H) / nm	*d*(H···A) / nm	*d*(D···A) / nm	∠DHA / (°)
1	O16−H16···O13	0.085(5)	0.217(3)	0.282 9(4)	135(5)
	O16−H16A···O13	0.084(4)	0.223(4)	0.282 9(4)	129(4)
	C2−H2A···O14	0.097 00	0.260	0.327 7(5)	127
	C9−H9···O12#2	0.093 00	0.234	0.324 7(5)	166
	C10−H10B···O14#2	0.097 00	0.256	0.334 2(5)	137
	C12−H12···O7#1	0.093 00	0.237	0.324 1(4)	157
	C16−H16B···O8#3	0.093 00	0.254	0.339 9(5)	153
	C22−H22F···O15#4	0.096 00	0.252	0.344 8(11)	163
	C11−H11A···Cg6	0.096 00	0.282	0.338 9(5)	119
2	O32−H32···O7	0.085(3)	0.236(4)	0.267 5(4)	102(3)
	O32#5−H32···O11#5	0.085(3)	0.207(3)	0.28 55(5)	153(4)
	C2−H2B···O12	0.097 00	0.236	0.307 5(5)	130
	C10−H10A···O8	0.097 00	0.241	0.334 0(5)	159
	C12−H12···O14#6	0.093 00	0.253	0.332 5(7)	144
	C10−H10B···O12#7	0.097 00	0.258	0.353 9(6)	169
	C19−H19B···O13	0.097 00	0.239	0.302 6(6)	122

Symmetry codes: #1: 2−*x*, 2−*y*, −*z*; #2: −1/2+*x*, 3/2−*y*, −1/2+*z*; #3: 2−*x*, 1−*y*, −*z*; #4: 1+*x*, *y*, *z* for **1**; #5: 1+*x*, *y*, *z*; #6: *x*, 1+*y*, *z*; #7: 1+*x*, 1+*y*, *z* for **2**.

interactions: O16–H16···O13, O16–H16A···O13, C2–H2A···O14, C9–H9···O12#2, C10–H10B···O14#2, C12–H12···O7#1, C16–H16B···O8#3 and C22–H22F···O15#4[58-61] (Table 3), which is shown in Fig.5 involving the coordinated ethanol molecule and NO_3^- ions in each molecule. There is also one intermolecular C–H···π (C11–H11A···Cg6) interaction. The molecule is interlinked through intermolecular C–H···π interactions into an infinite 1D chain (Fig.6).

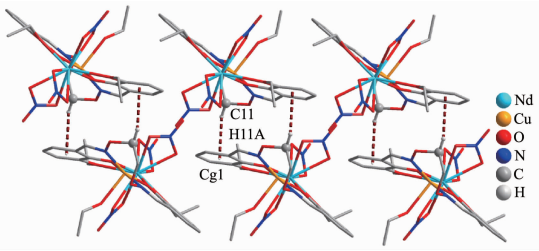

Symmetry codes: 2–x, 2–y, –z

Fig.6 View of intermolecular C–H···π interactions of complex **1**

2.4.2 Supramolecular interaction of complex **2**

In the crystal structure of complex **2**, there are seven intra- and inter-molecular hydrogen bond interactions: O32–H32···O7, O32#5–H32···O11#5, C2–H2B···O12, C10–H10A···O8, C10–H10B···O12#7, C12–H12···O14#6 and C19–H19B···O13#6, which are show in Table 3[62-66]. Due to the presence of the methanol molecule, hydrogen bonds constructed via the hydroxyl (Fig.7). The hydrogen bonds make the crystal structure of complex **2** more stable.

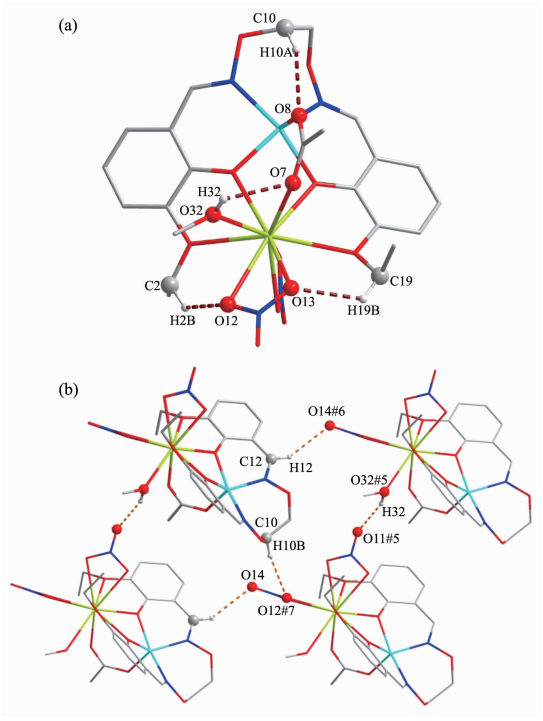

Symmetry codes: #5: 1+x, y, z; #6: x, 1+y, z; #7: 1+x, 1+y, z

Fig.7 (a) View of the intramolecular hydrogen-bonding interactions of complex **2**; (b) View of intermolecular interactions of complex **2**

2.5 Fluorescence properties

The fluorescence properties of H_2L and its complexes **1** and **2** were investigated in acetonitrile (10 μmol·L^{-1}) with excitation at 318 nm at room temperature (Fig.8). The ligand exhibited an intense emission peak at 384 nm, which should be assigned to the intraligand π-π* transition. The emission spectra of complex **2** showed one main peak at 389 nm (λ_{ex}= 318 nm). Meanwhile, it can be seen that complexes **1** and **2** exhibit a red-shift with respect to the ligand H_2L, which is tentatively assigned to a ligand-to-metal charge transfer (LMCT). In addition, compared with the emission spectrum of H_2L, the enhanced fluorescence intensity of complex **2** was observed, which is attributed to the following reasons: (1) the more rigidity of the ligand coordination to Zn(Ⅱ) ion that effectively reduces the loss of energy and increase the emission efficiency; (2) the full d^{10} electronic configuration of Zn(Ⅱ) ion; (3) an increased rigidity in structure of complex **2** and a restriction in the photo-induced electron transfer (PET)[67]. In addition, the differences of the peak positions may be considered to

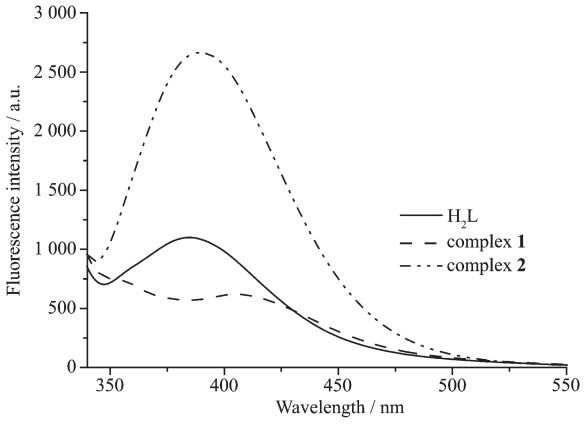

Fig.8 Emission spectra of H_2L and its complexes **1** and **2** in acetonitrile solutions (10 μmol·L^{-1}) at room temperature

be a result of the dissimilar coordination of the metal centers because the emission behavior is closely associated to the metal ions and ligand L^{2-} units around them. Compared with the free ligand H_2L, an extremely weak fluorescence intensity of complex **1** was observed, indicating that fluorescent characteristic has been influenced by the introduction of the Cu(Ⅱ) ion.

3 Conclusions

Two new heterobinuclear 3*d*-4*f* complexes were prepared by the one-pot reaction of a Salamo-type ligand H_2L with lanthanide (Ⅲ) nitrate and zinc (Ⅱ) acetate or copper(Ⅱ) acetate, respectively. The crystal structures of complexes **1** and **2** were confirmed by X-ray single crystal diffraction, and in complexes **1** and **2**, Cu(Ⅱ) and Zn(Ⅱ) ions are both penta-coordinated with a distorted square pyramidal geometry and the Nd (Ⅲ) and Ce (Ⅲ) ions are both deca-coordinated adopting a distorted bicapped twelve surface geometry.

Acknowledgements: This work was supported by the National Natural Science Foundation of China (Grants No. 21361015, 21761018) and the Program for Excellent Team of Scientific Research in Lanzhou Jiaotong University (Grant No. 201706), which is gratefully acknowledged.

References:

[1] Liu P P, Sheng L, Song X Q, et al. *Inorg. Chim. Acta*, **2015**, **434**:252-257

[2] Song X Q, Peng Y J, Chen G Q, et al. *Inorg. Chim. Acta*, **2015**,**427**:13-21

[3] Chen C Y, Zhang J W, Zhang Y H, et al. *J. Coord. Chem.*, **2015**,**68**:1054-1071

[4] Bunzli J C G, Piguet C. *Chem. Soc. Rev.*, **2005**,**34**:1048-1077

[5] Song X Q, Liu P P, Xiao Z R, et al. *Inorg. Chim. Acta*, **2015**, **438**:232-244

[6] Song X Q, Liu P P, Liu Y A, et al. *Dalton Trans.*, **2016**,**45**: 8154-8163

[7] Dong W K, Sun Y X, Xing S J, et al. *Z. Naturforsch.*, **2012**, **67b**:197-203

[8] Dong X Y, Gao L, Wang F, et al. *Crystals*, **2017**,**7**:267

[9] YANG Yu-Hua(杨玉华), HAO Jing(郝静), DONG Yin-Juan (董银娟), et al. *Chinese J. Inorg. Chem.*(无机化学学报), **2017**,**33**:1280-1292

[10]Dong Y J, Dong X Y, Dong W K, et al. *Polyhedron*, **2017**, **123**:305-315

[11]Dong X Y, Sun Y X, Wang L, et al. *J. Chem. Res.*, **2012**, **36**:387-390

[12]Xu L, Zhu L C, Ma J C, et al. *Z. Anorg. Allg. Chem.*, **2015**, **641**:2520-2524

[13]Song X Q, Cheng G Q, Wang X R, et al. *Inorg. Chim. Acta*, **2015**,**425**:145-153

[14]Dong X Y, Akogun S F, Zhou W M, et al. *J. Chin. Chem. Soc.*, **2017**,**64**:412-419

[15]Ma J C, Dong X Y, Dong W K, et al. *J. Coord. Chem.*, **2016**, **69**:149-159

[16]Chen L, Dong W K, Zhang H, et al. *Cryst. Growth Des.*, **2017**,**17**:3636-3648

[17]Zheng S S, Dong W K, Zhang Y, et al. *New J. Chem.*, **2017**, **41**:4966-4973

[18]Dong W K, Zhu L C, Dong Y J, et al. *Polyhedron*, **2016**, **117**:148-154

[19]Dong Y J, Li X L, Zhang Y, et al. *Supramol. Chem.*, **2017**, **29**:518-527

[20]Zhang H, Dong W K, Zhang Y, et al. *Polyhedron*, **2017**,**133**: 279-293

[21]Dong W K, Ma J C, Zhu L C, et al. *New J. Chem.*, **2016**,**40**: 6998-7010

[22]Li G, Hao J, Liu L Z, et al. *Crystals*, **2017**,**7**:217

[23]Liu P P, Wang C Y, Zhang M, et al. *Polyhedron*, **2017**,**129**: 133-140

[24]Liu Y A, Wang C Y, Zhang M, et al. *Polyhedron*, **2017**,**127**: 278-286

[25]Song X Q, Zheng Q F, Wang L, et al. *Luminescence*, **2012**, **25**:328-335

[26]Dong W K, Sun Y X, Zhao C Y, et al. *Polyhedron*, **2010**,**29**: 2087-2097

[27]Wang P, Zhao L. *Synth. React. Inorg. Met.-Org. Nano-Met. Chem.*, **2016**,**46**:1095-1101

[28]Hao J, Li L L, Zhang J T, et al. *Polyhedron*, **2017**,**134**:1-10

[29]Zhao L, Dang X T, Chen Q, et al. *Synth. React. Inorg. Met.-Org. Nano-Met. Chem.*, **2013**,**43**:1241-1246

[30]Sun Y X, Xu L, Zhao T H, et al. *Synth. React. Inorg. Met.-Org. Nano-Met. Chem.*, **2013**,**43**:509-513

[31]Sun Y X, Zhang S T, Ren Z L, et al. *Synth. React. Inorg. Met.-Org. Nano-Met. Chem.*, **2013**,**43**:995-1000

[32]Wu H L, Wang C P, Wang F, et al. *J. Chin. Chem. Soc.*, **2015**,**62**:1028-1034

[33]Wu H L, Bai Y C, Zhang Y H, et al. *J. Coord. Chem.*, **2014**, **67**:3054-3066

[34]Wu H L, Pan G L, Bai Y C, et al. *J. Photochem. Photobiol. B*, **2014**,**135**:33-43

[35]Wu H L, Pan G. L, Bai Y C, et al. *Res. Chem. Intermed.*, **2015**,**41**:3375-3388

[36]Chai L Q, Zhang K Y, Tang L J, et al. *Polyhedron*, **2017**, **130**:100-107

[37]Wu H L, Pan G L, Bai Y C, et al. *J. Chem. Res.*, **2014**,**38**: 211-217

[38]Dong W K, Ma J C, Dong Y J, et al. *Polyhedron*, **2016**,**115**: 228-235

[39]Wang L, Hao J, Zhai L X, et al. *Crystals*, **2017**,**7**:277

[40]Wang B J, Dong W K, Zhang Y, et al. *Sens. Actuators B*, **2017**,**247**:254-264

[41]Wang F, Gao L, Zhao Q, et al. *Spectrochim. Acta Part A*, **2018**,**190**:111-115

[42]Dong W K, Akogun S F, Zhang Y, et al. *Sens. Actuators B*, **2017**,**238**:723-734

[43]Dong W K, Li X L, Wang L, et al. *Sens. Actuators B*, **2016**, **229**:370-378

[44]Dong W K, Ma J C, Zhu L C, et al. *Inorg. Chim. Acta*, **2016**, **445**:140-148

[45]Dong X Y, Lan P F, Zhou W M, et al. *J. Coord. Chem.*, **2016**,**69**:1272-1283

[46]Wang L, Li X Y, Zhao Q, et al. *RSC Adv.*, **2017**,**7**:48730-48737

[47]Dong X Y, Li X Y, Liu L Z, et al. *RSC Adv.*, **2017**,**7**:48394-48403

[48]Dong W K, Ma J C, Zhu L C, et al. *Cryst. Growth Des.*, **2016**,**16**:6903-6914

[49]Wang L, Ma J C, Dong W K, et al. *Z. Anorg. Allg. Chem.*, **2016**,**642**:834-839

[50]Dong Y J, Ma J C, Zhu L C, et al. *J. Coord. Chem.*, **2017**, **70**:103-115

[51]Sabbatini N, Guardigli M, Lehn J M, et al. *Coord. Chem. Rev.*, **1993**,**123**:201

[52]Bazzicalupi C, Bencini A, Giorgi C, et al. *Chem. Commun.*, **2000**,**7**:561

[53]Akine S, Taniguchi T, Dong W K, et al. *J. Org. Chem.*, **2005**,**70**:1704-1711

[54](a)Sheldrick G M. *Acta Crystallogr. Sect. A*: *Found. Crystallogr.*, **2008**,**A64**:112-122

(b)Sheldrick G M. *Acta Crystallogr. Sect. C*: *Cryst. Struct. Commun.*, **2015**,**C71**:3-8

[55]Panja A, Shaikh N, Vojtisek P, et al. *New J. Chem.*, **2002**, **26**:1025-1028

[56]Wang P, Zhao L. *Spectrochim. Acta Part A*, **2015**,**135**:342-350

[57]Addison A W, Rao T N, Reedijk J, et al. *Dalton Trans.*, **1984**,7:1349-1356

[58]Gao L, Wang F, Zhao Q, et al. *Polyhedron*, **2018**,**139**:7-16

[59]DONG Wen-Kui(董文魁), WANG Li(王莉), SUN Yin-Xia(孙银霞), et al. *Chinese J. Inorg. Chem.*(无机化学学报), **2011**,27(2):372-376

[60]Sun Y X, Gao X H. *Synth. React. Inorg. Met.-Org. Nano-Met. Chem.*, **2011**,**41**:973-978

[61]Li L H, Dong W K, Zhang Y, et al. *Appl. Org. Chem.*, **2017**, **31**:e3818

[62]DONG Wen-Kui(董文魁), FENG Jian-Hua(冯建华), ZHANG Yü-Jie(张玉洁), et al. *Chinese J. Inorg. Chem.*(无机化学学报), **2011**,**27**:1865-1870

[63]Tao C H, Ma J C, Zhu L C, et al. *Polyhedron*, **2017**,**128**:38-45

[64]DONG Wen-Kui(董文魁), LÜ Zhong-Wu(吕忠武), SUN Yin-Xia(孙银霞), et al. *Chinese J. Inorg. Chem.*(无机化学学报), **2009**,**25**:1627-1634

[65]Li X Y, Chen L, Gao L, et al. *RSC Adv.*, **2017**,**7**:35905-35916

[66]Sun Y X, Wang L, Dong X Y, et al. *Synth. React. Inorg. Met.-Org. Nano-Met. Chem.*, **2013**,**43**:599-603

[67]Chai L Q, Wang G, Sun Y X, et al. *J. Coord. Chem.*, **2012**, **65**:1621-1631